

See discussions, stats, and author profiles for this publication at: <https://www.researchgate.net/publication/6951653>

# Ab Initio Vibrational Calculations for $\text{H}_2\text{SO}_4$ and $\text{H}_2\text{SO}_4 \cdot \text{H}_2\text{O}$ : Spectroscopy and the Nature of the Anharmonic Couplings

ARTICLE in THE JOURNAL OF PHYSICAL CHEMISTRY A · AUGUST 2005

Impact Factor: 2.69 · DOI: 10.1021/jp058110l · Source: PubMed

CITATIONS

67

READS

60

3 AUTHORS, INCLUDING:



Yifat Miller

Ben-Gurion University of the Negev

56 PUBLICATIONS 1,140 CITATIONS

SEE PROFILE



Galina M Chaban

NASA

76 PUBLICATIONS 2,390 CITATIONS

SEE PROFILE

# Ab Initio Vibrational Calculations for H<sub>2</sub>SO<sub>4</sub> and H<sub>2</sub>SO<sub>4</sub>·H<sub>2</sub>O: Spectroscopy and the Nature of the Anharmonic Couplings

Y. Miller,<sup>†</sup> G. M. Chaban,<sup>‡</sup> and R. B. Gerber<sup>\*,†,§</sup>

Department of Physical Chemistry and Fritz Haber Research Center, The Hebrew University, Jerusalem 91904, Israel, NASA Ames Research Center, Moffett Field, California 94035, U.S.A., and Department of Chemistry, University of California, Irvine, California 92697, U.S.A.

Received: March 30, 2005; In Final Form: May 19, 2005

Vibrational frequencies for fundamental, overtone, and combination excitations of sulfuric acid (H<sub>2</sub>SO<sub>4</sub>) and of sulfuric acid monohydrate cluster (H<sub>2</sub>SO<sub>4</sub>·H<sub>2</sub>O) are computed directly from ab initio MP2/TZP potential surface points using the correlation-corrected vibrational self-consistent field (CC-VSCF) method, which includes anharmonic effects. The results are compared with experiment. The computed transitions show in nearly all cases good agreement with experimental data and consistent improvement over the harmonic approximation. The CC-VSCF improvements over the harmonic approximation are largest for the overtone and combination excitations and for the OH stretching fundamental. The agreement between the calculations and experiment also supports the validity of the MP2/TZP potential surfaces. Anharmonic coupling between different vibrational modes is found to significantly affect the vibrational frequencies. Analysis of the mean magnitude of the anharmonic coupling interactions between different pairs of normal modes is carried out. The results suggest possible mechanisms for the internal flow of vibrational energy in H<sub>2</sub>SO<sub>4</sub> and H<sub>2</sub>SO<sub>4</sub>·H<sub>2</sub>O.

## I. Introduction

In the troposphere, sulfur is emitted mainly as sulfur dioxide (SO<sub>2</sub>), with small amounts of OCS, CS<sub>2</sub>, (CH<sub>3</sub>)<sub>2</sub>S, and H<sub>2</sub>S, and all these chemicals oxidize to sulfuric acid (H<sub>2</sub>SO<sub>4</sub>).<sup>1–3</sup> H<sub>2</sub>SO<sub>4</sub> plays an important role in the formation of tropospheric aerosols,<sup>4</sup> which by the evidence significantly affect the earth's climate.<sup>5</sup> Most of the sulfate found in precipitation is a result of the rain-out of hygroscopic cloud condensation nuclei involving SO<sub>3</sub> and H<sub>2</sub>SO<sub>4</sub>. In the troposphere, in the presence of water, H<sub>2</sub>SO<sub>4</sub> may exist in the form of hydrates: H<sub>2</sub>SO<sub>4</sub>·*n*H<sub>2</sub>O (*n* = 1–3).<sup>6</sup> In view of the above, the spectroscopy of H<sub>2</sub>SO<sub>4</sub> and H<sub>2</sub>SO<sub>4</sub>·H<sub>2</sub>O is of considerable interest.

Vibrational spectra of the gas-phase H<sub>2</sub>SO<sub>4</sub> have been studied experimentally<sup>7–10</sup> in some detail. Most of the fundamental frequencies of H<sub>2</sub>SO<sub>4</sub> have been identified in the IR region.<sup>7,8</sup> Experimental vibrational spectroscopy data of liquid H<sub>2</sub>SO<sub>4</sub> and of aqueous solutions of the acid also have been reported.<sup>11–26</sup> Most of these studies<sup>11–24</sup> used mainly IR spectroscopy; only a few<sup>25,26</sup> used Raman spectroscopy. The fundamental vibrational transitions of monomeric H<sub>2</sub>SO<sub>4</sub><sup>27,28</sup> and of its complex with water<sup>28</sup> were studied in matrix isolation conditions, and the mid-IR spectra were obtained. Recently, experimental and theoretical studies of the fundamental frequencies of H<sub>2</sub>SO<sub>4</sub> vapor were obtained by Hintze et al.<sup>29</sup> The overtone and combination transitions of H<sub>2</sub>SO<sub>4</sub> are weak and very difficult to observe experimentally, but Hintze et al.<sup>29,30</sup> and Feierabend et al.<sup>31,32</sup> were able to measure several overtone transitions and combination modes of H<sub>2</sub>SO<sub>4</sub>. So far, very few theoretical studies have been reported of the spectra of H<sub>2</sub>SO<sub>4</sub> and H<sub>2</sub>SO<sub>4</sub>·H<sub>2</sub>O, and

these all seem to use the harmonic approximation. Hintze et al.<sup>29</sup> calculated the harmonic fundamental transitions of H<sub>2</sub>SO<sub>4</sub> by using the density functional theory (DFT)/B3LYP method, whereas Natsheh et al.<sup>33</sup> used the DFT/PW91 method with the TZP basis set to compute the harmonic fundamental frequencies of H<sub>2</sub>SO<sub>4</sub> and H<sub>2</sub>SO<sub>4</sub> hydrates. Overtone OH stretching transitions for H<sub>2</sub>SO<sub>4</sub> and H<sub>2</sub>SO<sub>4</sub>·H<sub>2</sub>O were also computed using the local-mode model for the OH stretch.<sup>34</sup> This model is, however, not a first-principle calculation. We note that this approach is based on an ad hoc model. Since strong anharmonic effects can be expected for at least some of the transitions of H<sub>2</sub>SO<sub>4</sub> and H<sub>2</sub>SO<sub>4</sub>·H<sub>2</sub>O (e.g., the OH stretches), anharmonic calculations are obviously desirable. In the present study, we employ the correlation-corrected vibrational self-consistent field (CC-VSCF) approach to compute the fundamental, overtone, and combination excitations for H<sub>2</sub>SO<sub>4</sub> and H<sub>2</sub>SO<sub>4</sub>·H<sub>2</sub>O. Recently, we reported<sup>35</sup> applications of the ab initio CC-VSCF method to vibrational spectroscopy of HNO<sub>*x*</sub> molecules (*x* = 2, 3, 4) and HNO<sub>3</sub>·H<sub>2</sub>O.

The basic level of VSCF as an approximation for computing the anharmonic vibrational states of polyatomic systems was introduced by Bowman<sup>36,37</sup> and by Gerber and Ratner.<sup>38,39</sup> The CC-VSCF variant due to Jung and Gerber<sup>40</sup> and Norris et al.<sup>41</sup> provides corrections that significantly improve the accuracy of the standard VSCF approximation, while keeping the computational calculations relatively simple. Chaban et al.<sup>42</sup> combined the CC-VSCF algorithm with electronic structure methods, to yield ab initio CC-VSCF, an algorithm that directly computes the anharmonic vibrational states from an ab initio algorithm. In the present study, this version is employed, in order to use ab initio potential surfaces in the spectroscopic calculations. In fact, reliable anharmonic analytical force fields are not available, to our knowledge, for the systems targeted here. Thus, the advantages of the CC-VSCF method for the purpose of this

\* Corresponding author. Phone: 972-2-6585732. Fax: 972-2-6513742. E-mail: benny@fh.huji.ac.il.

<sup>†</sup> The Hebrew University.

<sup>‡</sup> NASA Ames Research Center.

<sup>§</sup> University of California.

study are as follows: (a) The method has proven to be of good accuracy in a range of applications to realistic systems.<sup>42–51</sup> (b) It directly employs ab initio potentials. (c) Computationally, the method is effective and applicable even with ab initio potentials for relatively large systems. For example, calculations for  $\text{H}_2\text{SO}_4 \cdot n\text{H}_2\text{O}$  for  $n = 2, 3$  are definitely feasible if desired in the future.

Although there have been many applications of VSCF for fundamental transitions, recently<sup>35</sup> the method also proved to be useful for overtone and combination excitations for realistic molecules described by ab initio MP2 potentials. Application of CC-VSCF for such excitations, in particular, for the large systems studied here, is a central objective of this work. Finally, the anharmonic interactions that are important for the vibrational spectroscopy calculations are also of major relevance to other properties of the systems, such as internal vibrational energy flow. The spectroscopic calculations establish the accuracy of the anharmonic interactions used, and an analysis of the properties of these potentials is carried out and reported here.

The structure of this paper is as follows. The methodology is presented in section II. Section III describes the results of the spectroscopic calculations, and the comparison with experimental frequencies is pursued in detail for all types of vibrational excitations. Section III also presents the analysis of the coupling strength calculations between normal modes in  $\text{H}_2\text{SO}_4$  and in  $\text{H}_2\text{SO}_4 \cdot \text{H}_2\text{O}$ . Conclusions are presented in section IV.

## II. Methodology

**A. The Vibrational Self-Consistent Field (VSCF) and Correlation-Corrected VSCF (CC-VSCF) Methods.** The VSCF method and the CC-VSCF variant have been described extensively in the literature.<sup>42–58</sup> Here, we give only a brief outline of the method. Before using the VSCF calculation, the equilibrium position, the harmonic frequencies, and the normal modes are computed. In the present study, the equilibrium geometry of the molecule of interest is optimized using an ab initio code analytic gradient of MP2/TZP energies.<sup>59,60</sup> Then, normal-mode analysis is performed for the equilibrium geometry by the standard procedure.<sup>61</sup>

The vibrational Schrödinger equation in mass-weighted normal-mode coordinates<sup>61</sup>  $Q_1, \dots, Q_N$  can be written as

$$\left[ -\frac{1}{2} \sum_{j=1}^N \frac{\partial^2}{\partial Q_j^2} + V(Q_1, \dots, Q_N) \right] \psi_n(Q_1, \dots, Q_N) = E_n \psi_n(Q_1, \dots, Q_N) \quad (1)$$

where  $V(Q_1, \dots, Q_N)$  is the full potential function for the system and  $N$  is the number of the vibrational normal modes. The method used here neglects rotation–vibration coupling effects. Equation 1 is subject to this approximation. For large molecules, this approximation should be justified. It is possible that coupling plays a role in the cases of  $\text{H}_2\text{SO}_4$  and  $\text{H}_2\text{SO}_4 \cdot \text{H}_2\text{O}$ .

The VSCF approximation is based on the ansatz

$$\psi_n(Q_1, \dots, Q_N) = \prod_{j=1}^N \psi_j^{(n)}(Q_j) \quad (2)$$

which leads to the single-mode VSCF equations

$$\left[ -\frac{1}{2} \frac{\partial^2}{\partial Q_j^2} + \bar{V}_j^{(n)}(Q_j) \right] \psi_j^{(n)}(Q_j) = \epsilon_j^{(n)} \psi_j^{(n)}(Q_j) \quad (3)$$

In the actual calculations, the wave functions  $\psi_j^{(n)}(Q_j)$  are

generated numerically on a grid. The effective VSCF potential for mode  $Q_j$  is given by

$$\bar{V}_j^{(n)}(Q_j) = \left\langle \prod_{l \neq j}^N \psi_l^{(n)}(Q_l) \middle| V(Q_1, \dots, Q_N) \middle| \prod_{l \neq j}^N \psi_l^{(n)}(Q_l) \right\rangle \quad (4)$$

Equations 3 and 4 for the single-mode wave functions, energies, and effective potentials must be solved self-consistently. The VSCF approximation for the total energy is then given by

$$E_n^{\text{VSCF}} = \sum_{j=1}^N \epsilon_j^{(n)} - (N-1) \left\langle \prod_{j=1}^N \psi_j^{(n)}(Q_j) \middle| V(Q_1, \dots, Q_N) \middle| \prod_{j=1}^N \psi_j^{(n)}(Q_j) \right\rangle \quad (5)$$

The CC-VSCF approach by Jung and Gerber<sup>40</sup> corrects the VSCF wave function for correlation effects between different vibrational modes by using second-order perturbation theory<sup>41</sup>

$$E_n^{\text{CC-VSCF}} = E_n^{\text{VSCF}} + \sum_{m \neq n} \frac{\left| \left\langle \prod_{j=1}^N \psi_j^{(n)}(Q_j) \middle| \Delta V \middle| \prod_{j=1}^N \psi_j^{(m)}(Q_j) \right\rangle \right|^2}{E_n^{(0)} - E_m^{(0)}} \quad (6)$$

where  $\Delta V$  is the difference between the true potential and the separable VSCF potential

$$\Delta V(Q_1, \dots, Q_N) = V(Q_1, \dots, Q_N) - \sum_{j=1}^N \bar{V}_j^{(n)}(Q_j) \quad (7)$$

By obtaining eq 6, the assumption is made that there is no excited-state degeneracy.  $E_n^{\text{VSCF}}$  is the total VSCF energy, given by eq 5, and

$$E_m^{(0)} = \sum_{j=1}^N \epsilon_j^{(n),m} \quad (8)$$

where  $\epsilon_j^{(n),m}$  is the  $m$ th SCF energy level of the  $j$ th mode, computed from the Hamiltonian

$$\bar{H}_n^{(n)}(Q_j) = -\frac{1}{2} \frac{\partial^2}{\partial Q_j^2} + \bar{V}_j^{(n)}(Q_j) \quad (9)$$

The second-order correlation-corrected treatment is important for having sufficient accuracy for systems such as those addressed here. Considerable experience points to the conclusion that, with relatively few exceptions of extremely anharmonic systems, this level of treatment is indeed quantitatively adequate for comparison with experiment.

**B. Approximation of Pairwise Interactions between the Normal Modes.** When the potential function is retained in full generality, the VSCF method involves prohibitively costly multidimensional integrals. Furthermore, the calculation of ab initio potential points for a full grid in  $N$ -dimensional space is not feasible for large  $N$ . There is, however, an approximation that avoids both difficulties. It is assumed that the potential function  $V(Q_1, \dots, Q_N)$  includes, in addition to the single-mode terms, only interactions between pairs of normal modes

$$V(Q_1, \dots, Q_N) = \sum_{j=1}^N V_j^{\text{diag}}(Q_j) + \sum_{i=1}^{N-1} \sum_{i < j}^N V_{ij}^{\text{coup}}(Q_i, Q_j) \quad (10)$$

This means that interaction terms involving the direct coupling of three or more normal modes are neglected. This approximation has proven successful in many applications.<sup>40,42–52,54,55</sup> It cannot, however, be taken for granted and must in principle be tested carefully in each application. Each term  $V_j^{\text{diag}}(Q_j)$  is equal to  $V(0, 0, \dots, Q_j, \dots, 0, 0)$ . The coupling terms for pairs of normal modes are given by

$$V_{ij}^{\text{coup}}(Q_i, Q_j) = V(0, \dots, Q_i, \dots, Q_j, \dots, 0) - V(0, \dots, Q_i, \dots, 0) - V(0, \dots, Q_j, \dots, 0) \quad (11)$$

In the present calculations,  $V_j^{\text{diag}}(Q_j)$  and  $V_{ij}^{\text{coup}}(Q_i, Q_j)$  are calculated directly from the ab initio program on eight-point grids along each normal coordinate and on  $8 \times 8$  grids for each pair of normal coordinates.

These potentials are interpolated into 16 and  $16 \times 16$  point grids. This technique was shown to work reasonably well in previous studies and to predict anharmonic frequencies for the stretching vibrations with the accuracy of  $30\text{--}50\text{ cm}^{-1}$  compared with experiment.<sup>43,48</sup> Note that in the framework of eq 10 there are two types of anharmonic interactions: the intrinsic anharmonicity of which mode, given by the  $V_j^{\text{diag}}(Q_j)$  and not involving any couplings between different modes, and the anharmonic mode–mode coupling term  $V_{ij}^{\text{coup}}(Q_i, Q_j)$ . These quantities will be explained and examined later for the systems studied here.

**C. Problem of Torsional Modes in VSCF.** The treatment of soft torsional modes in standard VSCF, which employs normal modes, often fails.<sup>40</sup> Soft torsional modes are adequately treated by angular (rotational) variables. A treatment by rectilinear normal modes leads to unphysically large coupling between the “torsional” normal mode and other modes. Therefore, VSCF and CC-VSCF usually give poor results. Although the results for the frequencies of the torsional modes themselves are often poor in these cases, in the systems studied so far this problem has not affected the accuracy of the frequencies of the other modes evaluated for the same systems, which is generally very good. A standard VSCF code with angular variables to describe soft torsions is as yet unavailable. However, the inapplicability of VSCF can be anticipated for each application from large, unphysical magnitudes of  $V_j^{\text{diag}}(Q_j)$  and  $V_{ij}^{\text{coup}}(Q_i, Q_j)$  ( $Q_j$  here is the “torsional” normal mode) or from unphysically large anharmonic “corrections” (20% and more) of the CC-VSCF calculations for the frequencies. The simplest remedy is just to retain the harmonic frequency value, when the VSCF calculations suggest the latter is inapplicable for the torsional mode. Thus, in the present study, the torsional transitions were treated harmonically.

**D. The Computational Implementation of the CC-VSCF Code.** The calculations using the CC-VSCF algorithm were done with the GAMESS package of programs,<sup>62</sup> in which CC-VSCF is implemented. The calculations were performed with the MP2 electronic structure method and the TZP basis set<sup>59,60</sup> that are not computationally very demanding. More accurate electronic structure algorithms (e.g., coupled clusters methods) and better basis sets (e.g., correlation-consistent basis sets) are obviously expected to provide more accurate potentials, including more accurate anharmonic couplings. Given the large number of potential surface points employed in CC-VSCF calculations, it is important not to use basis sets or electronic structure algorithms that are too costly. This level (MP2/TZP) was shown to provide anharmonic frequencies of reasonable quality as compared to experimental data.<sup>42–51</sup>

In this approach, the calculation of the overtone and combination modes is similar to that of the fundamentals and

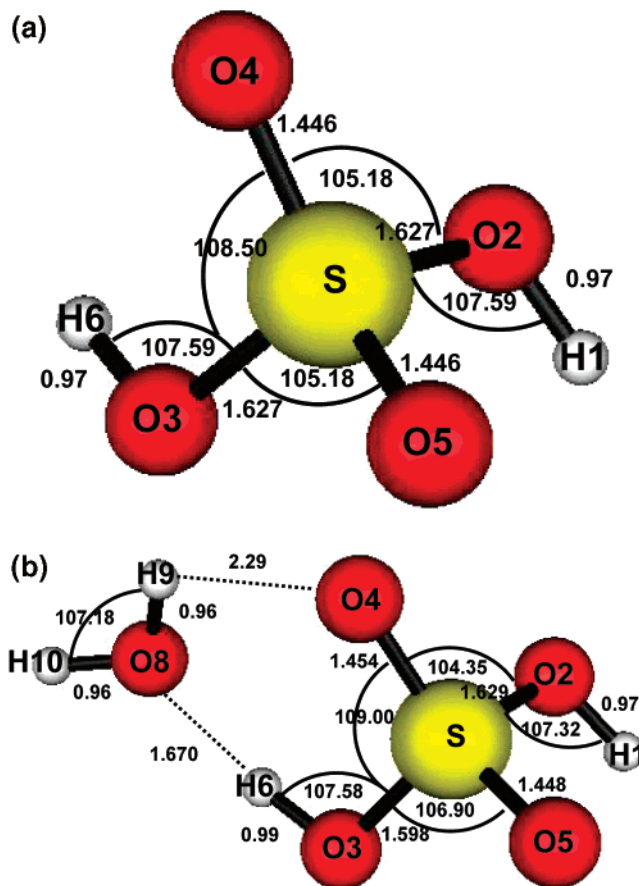


**Figure 1.** Optimized equilibrium structures of (a) H<sub>2</sub>SO<sub>4</sub> and (b) H<sub>2</sub>SO<sub>4</sub>·H<sub>2</sub>O. Bond lengths (in angstroms) and angles (in degrees) are given for the ab initio MP2/TZP level.

employs the same VSCF eqs 3–6, only the quantum numbers and effective potentials correspond to these cases. In overtone excitations, it is important to check that the number of grid points employed is sufficiently large to represent the very oscillatory excited-mode wave functions.

### III. Results and Discussion

**A. Structures.** The gas-phase sulfuric acid has two equilibrium structures: the trans and cis isomers. Natsheh et al.<sup>33</sup> calculated the total energy of these two structures by using the DFT/PW91 method with a TZP basis set. They reported that the difference between the total energy of these two structures is less than 1 kcal/mol and that the trans structure has the lower total energy. Figure 1a shows the equilibrium geometry of the trans structure of H<sub>2</sub>SO<sub>4</sub>, which was obtained in this study by the MP2/TZP method.<sup>59,60</sup> Table 1 presents the comparison of the computed geometrical parameters of H<sub>2</sub>SO<sub>4</sub> in this study with the experiment<sup>63</sup> and the comparison with an earlier theoretical study conducted by Natsheh et al.<sup>33</sup> The bond lengths and the angles obtained in this study are in agreement with those found by experiment as well as those of Natsheh et al.<sup>33</sup> In fact, the O1–H2 bond and the angles H1–O2–S and O2–S–O3 agree more closely with experiment than those of Natsheh et al.<sup>33</sup> The torsional angles in both theoretical studies have relatively large deviations from experimental values. On the whole, the computed geometrical parameters of H<sub>2</sub>SO<sub>4</sub> of these two theoretical studies are, however, in accord with experimental data. Natsheh et al.<sup>33</sup> claim that the TZP basis set gives better agreement with experiment than the theoretical study of Re



**TABLE 1: Comparisons of the Computed  $\text{H}_2\text{SO}_4$  Geometry with Theoretical Study by Natsheh et al.<sup>33</sup> and with Experimental Data**

parameter	DFT/PW91-TZP <sup>a</sup>	MP2/TZP	experiment <sup>b</sup>
R(O1-H2), Å	0.980	0.97	0.97 ± 0.01
R(O2-S), Å	1.626	1.627	1.574 ± 0.01
R(O4-S), Å	1.441	1.446	1.422 ± 0.01
∠(H1-O2-S), deg	106.5	107.59	108.5 ± 1.5
∠(O2-S-O4), deg		105.18	106.4 ± 0.5
∠(O3-S-O4), deg		108.50	108.6 ± 0.5
∠(O4-S-O5), deg	125.00	125.62	123.3 ± 1
∠(O2-S-O3), deg	102.3	101.33	101.3 ± 1
τ(H1-O2-S-O4), deg	25.4	30.08	20.08 ± 1
τ(H1-O2-S-O3), deg	-85.1	-80.32	-90.9 ± 1

<sup>a</sup> ref 33. <sup>b</sup> ref 62.**TABLE 2: Comparisons of the Computed  $\text{H}_2\text{SO}_4\cdot\text{H}_2\text{O}$  Geometry with Theoretical Study by Natsheh et al.<sup>33</sup> and with Experimental Data**

parameter	DFT/PW91-TZP <sup>a</sup>	MP2/TZP	experiment <sup>b</sup>
R(H1-O2), Å	0.98	0.97	0.95
R(O2-S), Å	1.63	1.629	1.578
R(O3-S), Å	1.59	1.598	1.567
R(O4-S), Å	1.46	1.454	1.464
R(O5-S), Å	1.44	1.448	1.410
R(H6-O3), Å	1.03	0.99	1.04
R(H6-O8), Å	1.61	1.670	1.645
R(H9-O8), Å		0.96	0.98
R(H10-O8), Å		0.96	0.98
∠(H1-O2-S), deg		107.32	108.5
∠(O2-S-O4), deg		104.35	104.71
∠(O3-S-O4), deg		109.00	106.71
∠(O3-S-O5), deg		106.90	106.7
∠(H6-O3-S), deg		107.58	108.6
∠(O4-S-O5), deg		123.98	123.3
∠(O2-S-O3), deg		102.32	101.8
∠(H9-O8-H10), deg		107.18	107

<sup>a</sup> ref 33. <sup>b</sup> ref 64.

et al.,<sup>64</sup> in which the B3LYP method and the D95++(d,p) basis set were used.

Three equilibrium molecular structures of the complex  $\text{H}_2\text{SO}_4\cdot\text{H}_2\text{O}$  were investigated:<sup>33</sup> the cis structure with a water molecule (c-SW), the trans structure with a water molecule (t-SWa), and another structure, which is relatively similar to the trans structure with a water molecule (t-SWb). The differences between the two latter structures (t-SWa and t-SWb) are in the orientation of the hydrogen bond of the water molecule and (a slight difference) in the O-H bond that is near the water molecule. The calculations in this study were performed for the trans structure with a water molecule (t-SWa), because it is the most stable structure and experimental data for this structure are available.<sup>28,65</sup> Figure 1b shows the equilibrium structure of  $\text{H}_2\text{SO}_4\cdot\text{H}_2\text{O}$ , which was obtained in this study by using the ab initio MP2/TZP level.<sup>59,60</sup> It should be noted that the stable structure is the neutral structure and not the ionic structure  $\text{H}_3\text{O}^+[\text{HSO}_4]^-$ . Comparison of the geometrical parameters of the  $\text{H}_2\text{SO}_4\cdot\text{H}_2\text{O}$  complex calculated in this study with those obtained by Natsheh et al.<sup>33</sup> and with an experimental study of Fiacco et al.<sup>65</sup> can be seen in Table 2. The calculated bond lengths in both theoretical methods are in very good agreement with experimental data. The percentages of deviation of the bond lengths from the experimental results in this study are less than 3.23%. The computed angles in this study also are in accord with experimental values. The percentages of deviations of the angles are less than 2.15%. Similarly, for  $\text{H}_2\text{SO}_4$ , the computed geometrical parameters using the MP2/TZP method are in better accord with the experiment than those obtained at the B3LYP/D95++(d,p) level by Re et al.<sup>64</sup>

**TABLE 3: Comparisons of the Fundamental Frequencies (in  $\text{cm}^{-1}$ ) of the  $\text{H}_2\text{SO}_4$  Molecule Obtained in This Study to the Theoretical Data of Natsheh et al.<sup>33</sup> and to Experimental Data**

mode	assignment	harmonic/ MP2-TZP	harmonic DFT/ PW91-TZP <sup>a</sup>	CC-VSCF/ MP2-TZP	expt
1	OH sym. str.	3819.96	3632	3589.54	3609.2 <sup>b</sup>
2	OH asy. str.	3815.49	3627	3499.51	
3	S=O <sub>2</sub> asy. str.	1456.17	1426	1434.33	1464.7 <sup>b</sup>
4	S=O <sub>2</sub> sym. str.	1196.95	1160	1182.67	1220.1 <sup>b</sup>
5	SOH asy. bend	1160.69	1153	1127.55	1157.1 <sup>b</sup>
6	SOH sym. bend	1149.91	1138	1118.16	1138 <sup>c</sup>
7	S(OH) <sub>2</sub> asy. str.	839.80	801	821.13	891.4 <sup>b</sup>
8	S(OH) <sub>2</sub> sym. str.	791.77	745	779.15	834.1 <sup>b</sup>
9	O-S=O rock	529.93	513	524.62	568 <sup>c</sup>
10	S=O <sub>2</sub> bend	511.70	499	518.78	550 <sup>c</sup>
11	S=O <sub>2</sub> wag	476.46	463	480.32	
12	O-S=O bend	426.32	413	488.70	
13	OH asy. torsion	368.47	341	378.70	281.1 <sup>d</sup>
14	O-S=O twist	320.57	321	458.81	
15	OH sym. torsion	259.76	221	379.60	215.7 <sup>d</sup>

<sup>a</sup> ref 33. <sup>b</sup> ref 29. <sup>c</sup> ref 7. <sup>d</sup> ref 32.

The  $\text{H}_2\text{SO}_4$  monomer has a  $C_2$  symmetric structure, whereas this symmetry is broken for  $\text{H}_2\text{SO}_4$  in the complex (Figure 1a and b). For example, the O3-H6 bond length in the complex, which is near the water molecule, increases as would be expected because of the effects of the hydrogen bonding.

### B. Vibrational Frequencies: Fundamental Transitions.

The fundamental transitions of  $\text{H}_2\text{SO}_4$ , obtained at the harmonic and CC-VSCF levels, using the MP2/TZP potential energy surface are shown in Table 3. The calculated fundamental frequencies for  $\text{H}_2\text{SO}_4$  computed here are also compared in Table 3 with the harmonic results, calculated by Natsheh et al.,<sup>33</sup> using the DFT/PW91 potential with a TZP basis set. The DFT harmonic calculations of Natsheh et al.<sup>33</sup> give better results than the present MP2 harmonic approximation for the OH symmetric stretching vibration. On the other hand, for the torsional modes and for the SOH symmetric stretch, the MP2 harmonic results are in better agreement with experiment than the harmonic results obtained by Natsheh et al.<sup>33</sup> The success of harmonic DFT in predicting experimental results for the OH symmetric stretch and torsional mode is, in our view, fortuitous: DFT harmonic frequencies are typically too soft. For the above-mentioned modes that are strongly anharmonic, this DFT error cancels partly with the error due to the harmonic approximation, yielding near-agreement with experiment. In our assessment, it is probably MP2 that gives more accurate potentials, but that can only be judged when anharmonic frequencies are computed.

We consider now the CC-VSCF anharmonic results that were computed here from the MP2 potentials. A major improvement is provided by the CC-VSCF method over the harmonic approximation for the OH symmetric stretching vibration. Experimental data for the OH asymmetric stretching vibration are not available. In a recent study,<sup>35</sup> we found that the anharmonic frequencies of the OH stretching vibrations for the  $\text{HNO}_x$  ( $x = 2, 3, 4$ ) and for  $\text{HNO}_3\cdot\text{H}_2\text{O}$  are in much better agreement with experiment than the harmonic approximation, and the results for  $\text{H}_2\text{SO}_4$  behave similarly. The calculated anharmonic value for the OH symmetric stretching vibration is in better agreement with the experiment than those obtained by Havey et al.<sup>66</sup> and Hintze et al.<sup>29</sup> Further improvements of the CC-VSCF method over the ab initio harmonic approximation are seen for the SOH symmetric bend and for the S=O<sub>2</sub> bend (see Table 3). For the other vibrational modes, the ab initio harmonic results are very slightly in closer agreement with experiment than the CC-VSCF method. The slight advantage

**TABLE 4: Comparisons of the Fundamental Frequencies (in cm<sup>-1</sup>) of the H<sub>2</sub>SO<sub>4</sub>·H<sub>2</sub>O Complex Obtained in This Study to the Theoretical Data of Natsheh et al.<sup>33</sup> and to Experimental Data**

mode	assignment	harmonic MP2/TZP	harmonic DFT/ PW91-TZP <sup>a</sup>	CC-VSCF/ MP2-TZP	experiment <sup>b</sup>
1	OH asy. str. of H <sub>2</sub> O	3985.76	3730	3737.83	3745.1
2	OH sym. str. of H <sub>2</sub> O	3840.92	3508	3593.20	3640.0
3	free OH str. of H <sub>2</sub> SO <sub>4</sub> (far from H <sub>2</sub> O molecule)	3822.33	3638	3627.80	3572.6
4	H-bonded OH str. of H <sub>2</sub> SO <sub>4</sub> (near H <sub>2</sub> O molecule)	3302.88	2771	2972.83	
5	HOH bend of H <sub>2</sub> O	1618.92	1607	1573.00	1599.7
6	O=S=O asy. str.	1468.32	1464	1436.40	1449.1
7		1368.04	1343	1336.23	
8	O=S=O sym. str.	1186.77	1140	1171.86	1204.8
9		1157.92	1131	1152.78	
10	S(OH) <sub>2</sub> asy. str.	884.40	917	867.52	887
11	S(OH) <sub>2</sub> sym. str.	820.39	856	834.05	834
12	SOH <sub>2</sub> asy. str.	790.01	761	787.30	
13	O-S=O rock	538.25	635	536.05	
14	intermolecular mode	527.29	527	540.42	
15	S=O <sub>2</sub> bend	504.17	509	514.14	
16	intermolecular mode	461.97	491	599.82	
17	O-S=O bend	415.91	411	485.54	
18	S=O <sub>2</sub> wag	382.92	389	476.21	
19	OH asy. torsion	348.58	339	528.81	554
20	OH sym. torsion	269.11	284	396.50	
21	intermolecular mode	231.41	258	331.35	
22	intermolecular mode	213.65	212	528.84	
23	intermolecular mode	126.20	167	180.21	
24	intermolecular mode	50.23	48	104.26	

<sup>a</sup> ref 33. <sup>b</sup> ref 28.

of the harmonic results in these cases is probably accidental, because of flaws in the MP2/TZP potentials.

Table 4 presents results for H<sub>2</sub>SO<sub>4</sub>·H<sub>2</sub>O: the harmonic frequencies obtained using the ab initio MP2/TZP potential, the DFT harmonic frequencies obtained by Natsheh et al.,<sup>33</sup> and the anharmonic frequencies obtained by the CC-VSCF method. We compare first the ab initio MP2/TZP harmonic results with the DFT/PW91-TZP harmonic calculations for the OH stretching vibrations of the water and of the H<sub>2</sub>SO<sub>4</sub> in the complex. As in the case of isolated H<sub>2</sub>SO<sub>4</sub>, the DFT harmonic calculation also gives better OH stretching frequencies for H<sub>2</sub>SO<sub>4</sub>·H<sub>2</sub>O than the harmonic MP2 calculations. As pointed out previously, this is probably due to the fact that the DFT method gives frequencies that are too soft, which cancel to a large extent with the error due to anharmonicity. We consider it probable that the MP2 potential surface is somewhat more accurate.

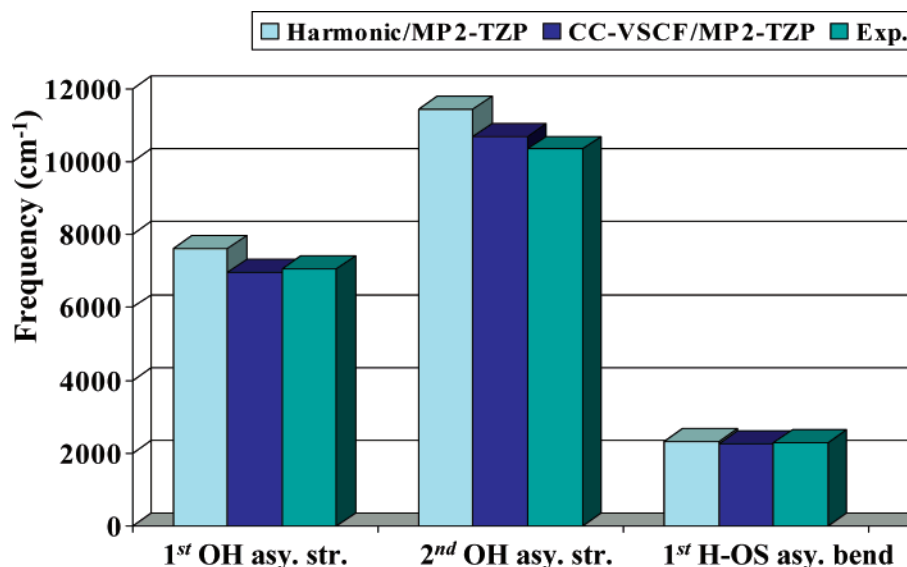
Consider now the anharmonic CC-VSCF results for H<sub>2</sub>SO<sub>4</sub>·H<sub>2</sub>O in Table 4. For most of the fundamental frequencies, the CC-VSCF approximation gives considerably better agreement with experiment than the harmonic approximation. The MP2 harmonic approximation gives better results than the CC-VSCF method by a relatively very small margin for only three vibrations: the HOH bend of the water molecule, the O=S=O asymmetric stretching vibration, and the S(OH)<sub>2</sub> asymmetric stretching vibration. Note that the anharmonic results are also in better agreement with experiment than the harmonic DFT results, except for the HOH bend of the water molecule. The interesting and surprising result of the CC-VSCF method is for the OH asymmetric torsion. Although treatment of the torsional mode by the CC-VSCF method often fails, in a case of the complex H<sub>2</sub>SO<sub>4</sub>·H<sub>2</sub>O, the result is in good accord with the experiment, whereas the harmonic frequency is off by 34%.

One of the improvements of the CC-VSCF method over the two harmonic approximation methods is for the OH stretching vibrations (Table 4). Moreover, experimental data for the H-bonded OH stretching vibration in H<sub>2</sub>SO<sub>4</sub>·H<sub>2</sub>O are not

available. Givan et al.<sup>28</sup> have drawn attention to the intriguing fact that this peak is not seen in their matrix. The calculated H-bonded OH stretching vibration obtained here is 2972.83 cm<sup>-1</sup>, and this peak is predicted to be very strong with an intensity of 1286.05 km/mol (Natsheh et al.<sup>33</sup> also reported that this peak is relatively very strong and that the absorption band of this peak is 2771 cm<sup>-1</sup>). No explanation is available at present as to why a peak systematically computed to be strong is not observed.

In summary, the following comments can be made about the fundamental transitions of H<sub>2</sub>SO<sub>4</sub> and H<sub>2</sub>SO<sub>4</sub>·H<sub>2</sub>O. The greatest improvement provided by the CC-VSCF method over the harmonic approximation is for the OH stretching vibrations. The very few values of transitions, in which the harmonic approximation results are better than CC-VSCF results (always by a small margin), could be accidental, because of the flaws of the MP2/TZP potential. Finally, the H<sub>2</sub>SO<sub>4</sub>·H<sub>2</sub>O complex is particularly challenging, because of the high anharmonicity of the weakly bound complex. Not surprisingly, for this strongly anharmonic system, the advantage of CC-VSCF over the harmonic approximation is greater than for H<sub>2</sub>SO<sub>4</sub>.

**C. Comparison of Calculations with Experiment: Overtone and Combination Modes.** Computing overtone and combination transitions for systems of more than several atoms, such as H<sub>2</sub>SO<sub>4</sub> and H<sub>2</sub>SO<sub>4</sub>·H<sub>2</sub>O, is quite challenging. Figure 2 shows the harmonic results and the CC-VSCF results for the first vibrational overtone excitations of the H-OS asymmetric bend and the OH asymmetric stretching vibration of H<sub>2</sub>SO<sub>4</sub> and also for the second vibrational overtone transition of the OH asymmetric stretching mode. The calculations are compared with the experimental data. The CC-VSCF results are in accord with the experiment for *all* the overtone transitions. The deviations of the first overtone excitation of the H-OS asymmetric stretching vibration, the first overtone of the OH asymmetric stretching vibration, and the second overtone of the OH asymmetric stretching vibration are ~25, ~99, and ~353 cm<sup>-1</sup>,

Figure 2. Overtone excitation frequencies (cm<sup>-1</sup>) for H<sub>2</sub>SO<sub>4</sub>.TABLE 5: Combination Frequencies (in cm<sup>-1</sup>) of H<sub>2</sub>SO<sub>4</sub>

mode 1	mode 2	combination mode	harmonic/MP2-TZP	CC-VSCF/MP2-TZP	experiment
OH asy. str.	H-OS asy. bend	$\nu_2 + \nu_5$	4976.18	4627.06	4739 <sup>a</sup>
first overtone of OH asy. str.	H-OS asy. bend	$2\nu_2 + \nu_5$	8791.66	8089.08	8163 <sup>a</sup>
OH asy. str.	OH sym. torsion	$\nu_2 + \nu_{15}$	4075.25	3879.11	3825.1 <sup>b</sup>
OH asy. str.	OH sym. torsion	$\nu_2 - \nu_{15}$	3555.73	3119.91	3393.9 <sup>b</sup>
OH asy. str.	OH asy. torsion	$\nu_2 + \nu_{13}$	4183.96	3878.21	3890.3 <sup>b</sup>
OH asy. str.	OH asy. torsion	$\nu_2 - \nu_{13}$	3447.02	3120.81	3328.5 <sup>b</sup>

<sup>a</sup> ref 29. <sup>b</sup> ref 30.TABLE 6: Comparison between  $\Delta E_{\text{diag}}$  (in cm<sup>-1</sup>) and  $\Delta E_{\text{coup}}$  (in cm<sup>-1</sup>) in H<sub>2</sub>SO<sub>4</sub>

mode	harmonic	diagonal	CC-VSCF	$\Delta E_{\text{diag}}$	$\Delta E_{\text{coup}}$
OH sym. str.	3819.96	3738.66	3589.54	-81.3	-149.12
OH asy. str.	3815.49	3909.03	3499.51	93.54	-409.52
S=O <sub>2</sub> asy. str.	1456.17	1462.59	1434.33	6.42	-28.26
S=O <sub>2</sub> sym. str.	1196.95	1193.82	1182.67	-3.13	-11.15
SOH asy. bend	1160.69	1194.16	1127.55	33.47	-66.61
SOH sym. bend	1149.91	1189.52	1118.16	39.61	-71.36
S(OH) <sub>2</sub> asy. str.	839.80	845.71	821.13	5.91	-24.58
S(OH) <sub>2</sub> sym. str.	791.77	788.36	779.15	-3.41	-9.21
O-S=O rock	529.93	530.09	524.62	0.16	-5.47
S=O <sub>2</sub> bend	511.70	512.89	518.78	1.19	5.89
S=O <sub>2</sub> wag	476.46	480.93	480.32	4.47	-0.61
O-S=O bend	426.32	486.52	488.70	60.2	2.18
OH asy. torsion	368.47	370.47	378.70	2	8.23
O-S=O twist	320.57	604.01	458.81	283.44	-145.2
OH sym. torsion	259.76	437.75	379.60	177.99	-58.15

respectively. On the other hand, the deviations for the harmonic approximation for these transitions are ~43, ~570, and ~1096 cm<sup>-1</sup>, respectively (see Figure 2). The improvement of the CC-VSCF over the harmonic approximation for overtone transitions is thus very large. Experimental data for the third and fourth overtone transitions for H<sub>2</sub>SO<sub>4</sub> have not yet been reported. However, in our recent study,<sup>35</sup> we demonstrated the application of the CC-VSCF method for computing high overtone excitations, that is, third and fourth overtone transitions of HNO<sub>3</sub> and HNO<sub>4</sub>. The above results suggest the desirability of further applications of VSCF for overtone excitations for other systems. We note that these calculations use ab initio potentials and are not limited to specific models of the vibrational Hamiltonian.

Combination-mode excitations, in a similar manner to overtone transitions, involve anharmonic interaction effects much stronger than the fundamental transitions, and the CC-

TABLE 7: Comparison between  $\Delta E_{\text{diag}}$  (in cm<sup>-1</sup>) and  $\Delta E_{\text{coup}}$  (in cm<sup>-1</sup>) in H<sub>2</sub>SO<sub>4</sub>·H<sub>2</sub>O

mode	harmonic	diagonal	CC-VSCF	$\Delta E_{\text{diag}}$	$\Delta E_{\text{coup}}$
OH asy. str. of H <sub>2</sub> O	3985.76	4021.24	3737.83	35.48	-283.41
OH sym. str. of H <sub>2</sub> O	3840.92	3749.76	3593.20	-91.16	-156.56
free OH str. of H <sub>2</sub> SO <sub>4</sub> (far from H <sub>2</sub> O molecule)	3822.33	3661.44	3627.80	-160.89	-33.64
H-bonded OH str. of H <sub>2</sub> SO <sub>4</sub> (near H <sub>2</sub> O molecule)	3302.88	3013.76	2972.83	-289.12	-40.93
HOH bend of H <sub>2</sub> O	1618.92	1614.77	1573.00	-4.15	-41.77
O=S=O asy. str.	1468.32	1477.25	1436.40	8.93	-40.85
	1368.04	1377.62	1336.23	9.58	-41.39
O=S=O sym. str.	1186.77	1185.08	1171.86	-1.69	-13.22
	1157.92	1213.59	1152.78	55.67	-60.81
S(OH) <sub>2</sub> asy. str.	884.40	884.19	867.52	-0.21	-16.67
S(OH) <sub>2</sub> sym. str.	820.39	873.35	834.05	52.96	-39.3
SOH <sub>2</sub> asy. str.	790.01	815.1	787.30	25.09	-27.8
O-S=O rock	538.25	538.44	536.05	0.19	-2.39
intermolecular mode	527.29	529.82	540.42	2.53	10.6
S=O <sub>2</sub> bend	504.17	506.45	514.14	2.28	7.69
intermolecular mode	461.97	624.63	599.82	162.66	-24.81
O-S=O bend	415.91	460.23	485.54	44.32	25.31
S=O <sub>2</sub> wag	382.92	442.86	476.21	59.94	33.35
OH asy. torsion	348.58	541.49	528.81	192.91	-12.68
OH sym. torsion	269.11	522.98	396.50	253.87	-126.48
intermolecular mode	231.41	267.46	331.35	36.05	63.89
intermolecular mode	213.65	559.57	528.84	345.92	-30.73
intermolecular mode	126.20	146.57	180.21	20.37	33.64
intermolecular mode	50.23	70.55	104.26	20.32	33.71

VSCF method seems an appropriate tool for computing these transitions. Recently, combination transitions for several systems were computed<sup>35,67</sup> by the CC-VSCF approximation, and the performance of the method has already been tested with encouraging results. Combination transitions which were computed directly from VSCF calculations were found quite close to those computed more approximately by adding CC-VSCF frequencies for the two corresponding single-mode transitions. Therefore, in this work, the combination transitions were

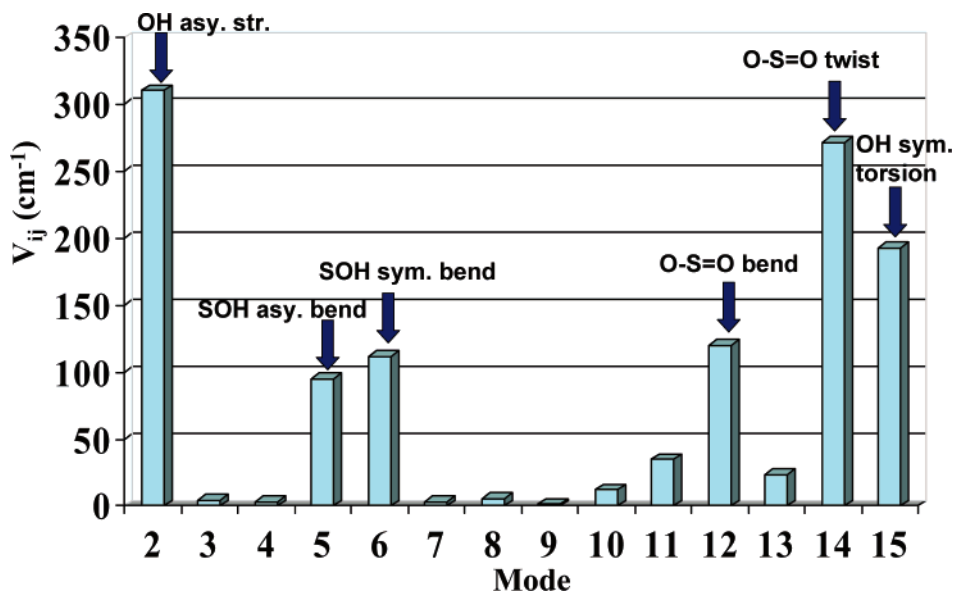


Figure 3. Magnitude of the coupling integral between the OH symmetric stretching vibration and the other modes in H<sub>2</sub>SO<sub>4</sub>.

obtained by the latter method. The comparison between the harmonic combination frequencies and the anharmonic for H<sub>2</sub>SO<sub>4</sub> are listed in Table 5. The MP2/TZP potential is used. The CC-VSCF results are in considerably better agreement with experiment than the harmonic ones. The largest improvements provided by the CC-VSCF method over the harmonic approximation are for the combination mode involving the OH asymmetric stretching vibration and the H–OS asymmetric bend and also for the combination mode of the first overtone excitation of the OH asymmetric stretching vibration and the fundamental transition of the H–OS asymmetric bend (Table 5). For the combination mode 1–1 of the OH asymmetric stretching vibration and the symmetric torsion, the percentage of deviation from experiment of the harmonic approximation is 4.8%, while that of the CC-VSCF is 8.1%. We think this result is accidental and caused by partial cancellation of errors associated with the potential and with the harmonic approximation.

**D. Intrinsic Single-Mode Anharmonicities versus Coupling between Modes.** As eq 11 shows, there are two different causes for anharmonic behavior: the intrinsic anharmonicity of mode, described by  $V_j^{\text{diag}}(Q_j)$ , and the anharmonic coupling between different modes  $V_{ij}^{\text{coup}}(Q_i, Q_j)$ . The contribution of the intrinsic single-mode anharmonicity ( $\Delta E_{\text{diag}}$ ) to the frequency is calculated as the difference between the frequency given by the diagonal potential  $V_j^{\text{diag}}(Q_j)$  and the harmonic value of the frequency, while the contribution of the anharmonic coupling element between modes ( $\Delta E_{\text{coup}}$ ) is computed as the difference between the CC-VSCF value and the frequency value  $V_j^{\text{diag}}(Q_j)$ . Comparison of the values  $\Delta E_{\text{diag}}$  and  $\Delta E_{\text{coup}}$  for each fundamental transition in H<sub>2</sub>SO<sub>4</sub> are shown in Table 6. The absolute values of  $\Delta E_{\text{coup}}$  in most of the vibrational modes are larger than the absolute values of  $\Delta E_{\text{diag}}$ , that is, the contribution of the anharmonic coupling between different modes is greater than that of the intrinsic single-mode anharmonicities. In several cases, such as OH asymmetric torsion, the contribution of the coupling potentials to the fundamental frequency is very small (8.23), but still greater than the intrinsic single-mode anharmonicity. Only for relatively few cases of four soft modes (S=O<sub>2</sub> wag, O=S=O bend, O=S=O twist, and OH symmetric torsion) is the contribution of the intrinsic single-mode anharmonicity larger than those of the coupling potentials. The comparison of the values  $\Delta E_{\text{diag}}$  and  $\Delta E_{\text{coup}}$  to each fundamental transition in

H<sub>2</sub>SO<sub>4</sub>·H<sub>2</sub>O can be seen in Table 7. Also in the case of H<sub>2</sub>SO<sub>4</sub>·H<sub>2</sub>O, the absolute values of  $\Delta E_{\text{coup}}$  are for most vibrational modes larger than  $\Delta E_{\text{diag}}$ . For a few vibrational modes only, the magnitudes of  $\Delta E_{\text{diag}}$  are greater than the corresponding  $\Delta E_{\text{coup}}$ . In summary, it appears that, for most transitions of the systems studied, the anharmonic couplings between different modes are larger than the intrinsic single-mode anharmonicities.

#### E. Magnitudes of Anharmonic Couplings between Modes.

The anharmonic couplings between different modes are of considerable interest. In addition to the effect on frequencies, these couplings govern, for example, the flow of vibrational energy between different normal modes in dynamical processes. There is, of course, no energy flow between normal modes in the harmonic approximation, nor can the  $V^{\text{diag}}$  potential terms cause energy flow in dynamics. Therefore, we use here certain quantities to characterize the magnitude of coupling between modes and analyze their behavior. The average absolute value of the coupling potential has already been studied for the six amino acid conformers.<sup>54</sup> It is useful to employ a quantity that involves the absolute value of the coupling potential; otherwise, cancellation of average quantities could be misleading as to the local magnitude of the couplings effects. We note that both the magnitude and the sign of the couplings are of importance for obtaining correct frequencies. We focus here, however, on the magnitudes which of the greatest physical importance. The definition used is therefore the average absolute value of the coupling potential, given by

$$\overline{V_{ij}}(Q_i, Q_j) = \langle \Psi_i(Q_i) \Psi_j(Q_j) | V_{ij}(Q_i, Q_j) | \Psi_i(Q_i) \Psi_j(Q_j) \rangle \quad (12)$$

where  $Q_i$  and  $Q_j$  are the normal-mode coordinates for modes  $i$  and  $j$ , and  $\Psi_i$  and  $\Psi_j$  are the ground-state wave functions. The wave functions enable us to set the range of the important points which are considered in the calculations. The integral is evaluated numerically as an integral over the grid points which are used in VSCF calculations.

The magnitude of the coupling integral between the OH symmetric stretching vibration with the other normal modes in H<sub>2</sub>SO<sub>4</sub> is shown in Figure 3, using the MP2/TZP potential. Figure 4 presents the magnitude of the coupling integral between the OH asymmetric stretching vibration with the other normal modes in H<sub>2</sub>SO<sub>4</sub>, using the MP2/TZP potential. As shown from Figures 3 and 4, the strong couplings of the OH stretching



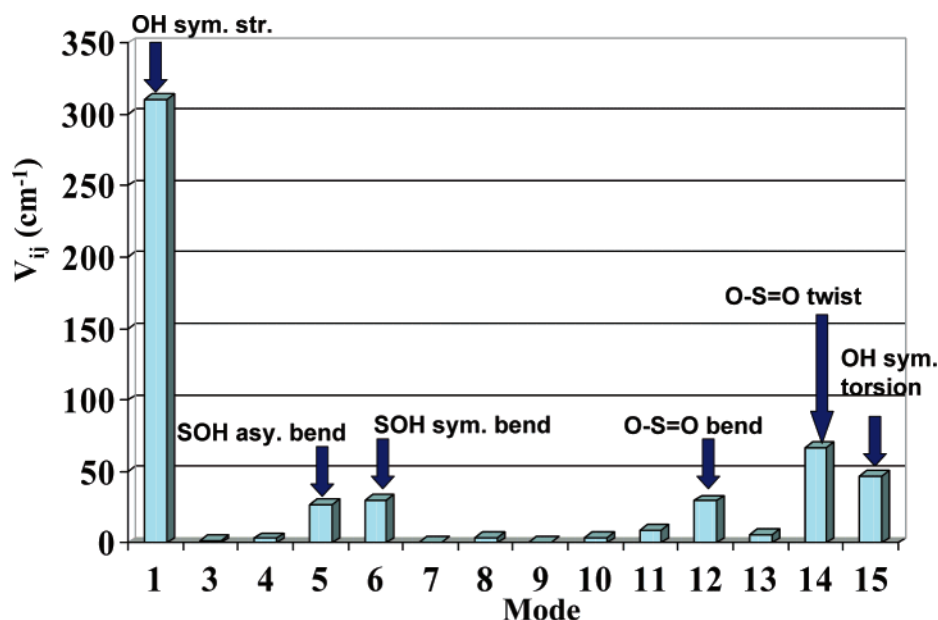


Figure 4. Magnitude of the coupling integral between the OH asymmetric stretching vibration and the other modes in  $\text{H}_2\text{SO}_4$ .

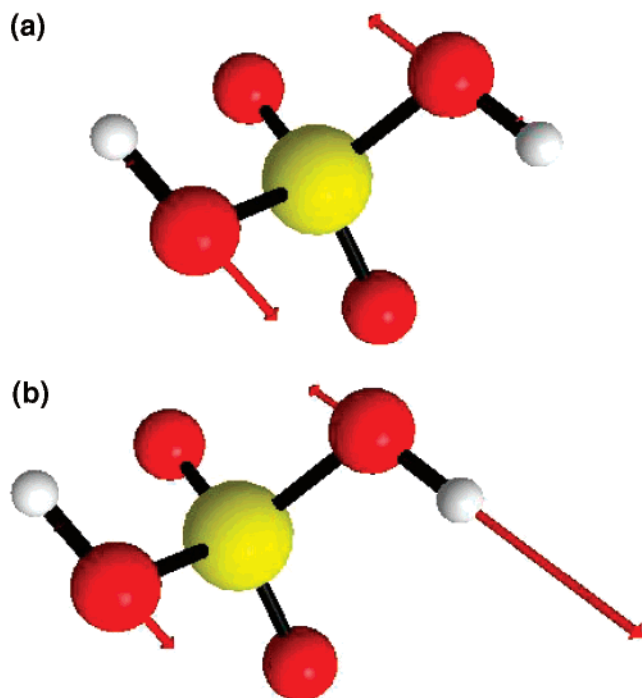


Figure 5. Vibrational modes of the (a) OH symmetric stretching and (b) the OH asymmetric stretching in  $\text{H}_2\text{SO}_4$ .

vibrational modes are with mode 5 (SOH asymmetric bend), mode 6 (SOH symmetric bend), mode 12 (O=S=O bend), mode 14 (O=S=O twist), and mode 15 (OH symmetric torsion). The largest magnitude of the coupling integral is between the OH asymmetric stretching vibration and the OH symmetric stretching vibration. The motions of these vibrations incorporate the same O and H atoms in  $\text{H}_2\text{SO}_4$ , as seen from Figure 5. As we found, anharmonic couplings between normal modes that involve the displacements of the same atoms are typically stronger.

Mode coupling is essential in the analysis of intramolecular vibrational energy redistribution (IVR). Feierabend et al.<sup>32</sup> gave experimental evidence for significant coupling between OH stretching vibrations and other modes in  $\text{H}_2\text{SO}_4$  (and  $\text{HNO}_3$ ), such as the OH symmetric torsional mode, SOH symmetric

bend, and OH asymmetric torsion. The OH symmetric torsional mode and SOH symmetric bend are coupled with the OH stretching vibrations; the OH asymmetric torsion (mode 13) is weakly coupled with the OH stretching vibration (Figures 3 and 4). Dynamics simulations of intermolecular energy flow are currently under study in our group. Tentative results show efficient energy flow from the OH asymmetric stretching vibration into the OH asymmetric torsional mode. The SOH symmetry bend (mode 6) also coupled with the OH stretching vibrations. Also, the dynamics simulations of internal energy flow show that energy transfers rapidly from the SOH asymmetry bend into the SOH symmetric bend. The magnitude of the coupling integral between these two vibrations is  $215\text{ cm}^{-1}$ , which is a strong coupling. Note that in addition to the strong coupling there is a 1:1 Fermi resonance between these two vibrations (see Table 3), which can also affect energy flow dynamics. Figures 6 and 7 present the magnitude of the coupling integral of the other normal modes in  $\text{H}_2\text{SO}_4\cdot\text{H}_2\text{O}$  with the free OH stretching vibration and the H-bonded OH stretching vibration, respectively. Each type of OH stretching vibration of  $\text{H}_2\text{SO}_4$  in the complex is coupled preferentially with different vibrations. The common aspect of these two OH stretching vibrations and the other vibrations to which they are coupled is that the same atoms participate in the motion for all these modes. The results on pair couplings show that the couplings between different normal modes depend strongly on the modes involved and are highly specific. This may have important implications for internal energy flow. In a current study in our group of dynamics simulations of internal energy flow, an analysis of the IVR of the complex shows quite efficient energy flow between the vibrations, including the intermolecular vibrations. In summary, analysis of the mean coupling strengths between different modes appear be useful for understanding both spectroscopy and intramolecular dynamics.

#### IV. Concluding Remarks

The vibrational spectra of  $\text{H}_2\text{SO}_4$  and  $\text{H}_2\text{SO}_4\cdot\text{H}_2\text{O}$  were studied by computing ab initio MP2 potential energy points (with TZP basis set) and using the CC-VSCF approach. The computed fundamental, overtone, and combination transition frequencies for both  $\text{H}_2\text{SO}_4$  and  $\text{H}_2\text{SO}_4\cdot\text{H}_2\text{O}$  are in good agreement with experimental data. These results support the

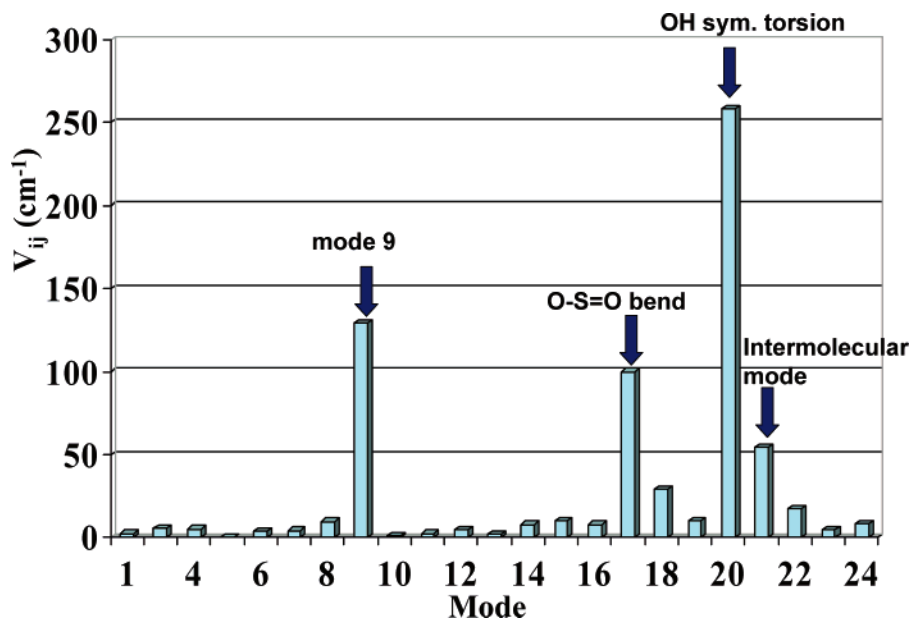


**Figure 6.** Magnitude of the coupling integral between the free OH stretching vibration (far from  $\text{H}_2\text{O}$  molecule) and the other modes in  $\text{H}_2\text{SO}_4\cdot\text{H}_2\text{O}$ .

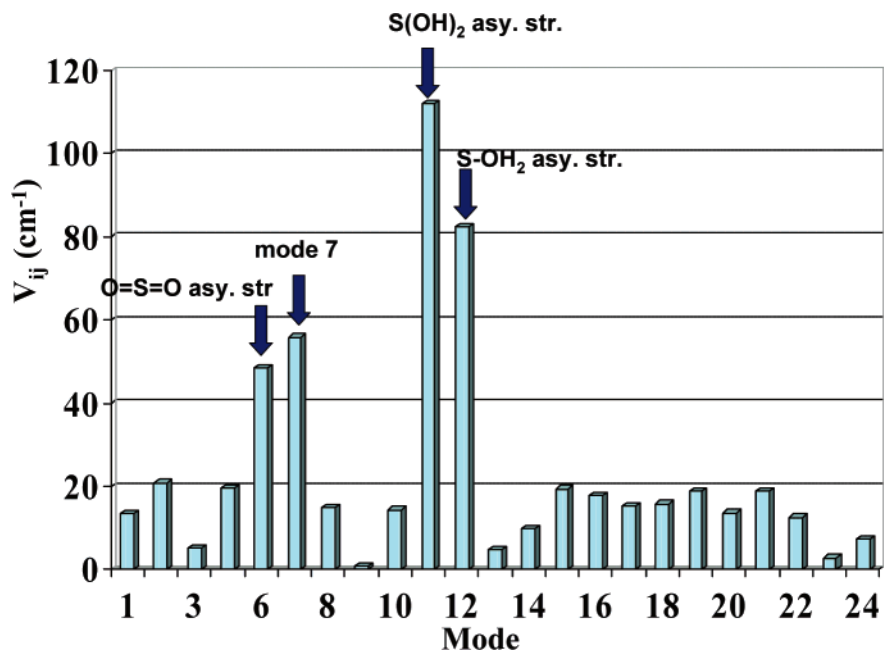


**Figure 7.** Magnitude of the coupling integral between the H-bonded OH stretching vibration (near  $\text{H}_2\text{O}$  molecule) and the other modes in  $\text{H}_2\text{SO}_4\cdot\text{H}_2\text{O}$ .

usefulness of the ab initio potentials for such systems (and also the validity of the VSCF method). The merit of using the ab initio potentials is that these realistic force fields are generally available and free of the bias of fitting or of arbitrary modeling.

Encouraged by the spectroscopic support for the quality of the potentials used, a study of quantities representing average coupling strengths between different normal modes was performed. The magnitudes of the anharmonic couplings were found to depend greatly on the nature of the modes involved and to be largest between modes involving significant displacements of the same atoms. Also, analysis of the spectroscopic quantities indicates that, for most transitions, anharmonic coupling between modes, rather than intrinsic anharmonicity of a single mode, is the dominant factor for the anharmonic effect. It is hoped to extend the anharmonic CC-VSCF spectroscopic calculations for additional and larger molecules

and complexes and to focus further on the properties of anharmonic coupling and also their role in dynamics.

**Acknowledgment.** We thank Dr. B. Brauer for her helpful comments. We also thank Professor B. J. Finlayson-Pitts and Professor A. Loewenschuss for their useful remarks, and Professor V. Vaida for providing her experimental results for overtone and combination of sulfuric acid. We also thank Professors S. A. Nizkorodov, H. G. Kjaergaard, P. Jungwirth, and L. F. Phillips for helpful discussion. This research was supported by the NSF, through the Environmental Molecular Science Institute at UC Irvine (NSF 0431312) and through the CRC project NSF CHE-0209719.

## References and Notes

- (1) Brasseur, G.; Solomon, S. *Aeronomy of the Middle Atmosphere*; Riedel: Dordrecht, The Netherlands, 1984.

- (2) Burkholder, J. B.; Mills, M.; McKeen, S. *Geophys. Res. Lett.* **2000**, 27, 2493.
- (3) Turco, R. P.; Whitten, R. C.; Toon, O. B. *Rev. Geophys. Space Phys.* **1982**, 20, 233.
- (4) D'Almeida, G. A.; Koepke, P.; Shettle, E. P. A. *Atmospheric Aerosols: Global Climatology and Radiative Characteristics*; Deepak Publishing: Hampton, VA, 1991.
- (5) Swartz, E.; Shi, Q.; Davidovits, P.; Jayne, J. T.; Wormsnop, D. R.; Kolb, C. E. *J. Phys. Chem. A* **1999**, 103, 8824.
- (6) Jaeger-Voirol, A.; Mirabel, P.; Reiss, H. *J. Chem. Phys.* **1987**, 87, 4849.
- (7) Chackalackal, S. M.; Stafford, F. E. *J. Am. Chem. Soc.* **1966**, 88, 723.
- (8) Stopperka, K.; Kilz, F. Z. *Anorg. Allg. Chem.* **1969**, 370, 49.
- (9) Majkowski, R. F.; Blint, R. J.; Hill, J. C. *Appl. Opt.* **1978**, 17, 975.
- (10) Eng, R. S.; Petagana, G.; Nill, K. W. *Appl. Opt.* **1978**, 11, 1723.
- (11) Giguere, P. A.; Savoie, R. *Can. J. Chem.* **1960**, 38, 2467.
- (12) Walrafen, G. E.; Dodd, D. M. *Trans. Faraday Soc.* **1961**, 57, 1286.
- (13) Gillespie, R. J.; Robinson, E. A. *Can. J. Chem.* **1962**, 40, 644.
- (14) Giguere, P. A.; Savoie, R. *J. Am. Chem. Soc.* **1963**, 85.
- (15) Stopperka, K.; Kilz, F. Z. *Z. Anorg. Allg. Chem.* **1969**, 370, 80.
- (16) Myhre, C. E. L. Canadian Scientist Thesis, University of Oslo, 1996.
- (17) Iraci, L. T.; Middlebrook, A. M.; Wilson, M. A.; Tolbert, M. A. *Geophys. Res. Lett.* **1994**, 21, 867.
- (18) Iraci, L. T.; Middlebrook, A. M.; Tolbert, M. A. *J. Geophys. Res., [Atmos.]* **1995**, 100, 20969.
- (19) Anthony, S. E.; Tisdale, R. T.; Disselkamp, R. S.; Tolbert, M. A.; Wilson, J. C. *Geophys. Res. Lett.* **1995**, 22, 1105.
- (20) Schindler, L. R.; Roberts, J. T. *J. Phys. Chem.* **1996**, 100, 19582.
- (21) Bertram, A. K.; Patterson, D. D.; Sloan, J. J. *J. Phys. Chem.* **1996**, 100, 2376.
- (22) Martin, S. T.; Salcedo, D.; Molina, L. T.; Molina, M. J. *J. Phys. Chem. B* **1997**, 101, 5307.
- (23) Anthony, S. E.; Onasch, T. B.; Tisdale, R. T.; Disselkamp, R. S.; Tolbert, M. A.; Wilson, J. C. *J. Geophys. Res., [Atmos.]* **1997**, 102, 10777.
- (24) Nash, K. L.; Sully, K. J.; Horn, A. B. *J. Phys. Chem. A* **2001**, 105, 9422.
- (25) Tomikawa, K.; Kanno, H. *J. Phys. Chem. A* **1998**, 102, 6082.
- (26) Myhre, C. E. L.; Christensen, D. H.; Nicolaisen, F. M.; Nielsen, C. J. *J. Phys. Chem. A* **2003**, 107, 1979.
- (27) Givan, A.; Larsen, L. A.; Loewenschuss, A.; Nielsen, C. J. *J. Mol. Struct.* **1999**, 509, 35.
- (28) Givan, A.; Larsen, L. A.; Loewenschuss, A.; Nielsen, C. J. *J. Chem. Soc., Faraday Trans.* **1998**, 94, 827.
- (29) Hintze, P. E.; Kjaergaard, H. G.; Vaida, V.; Burkholder, J. B. *J. Phys. Chem. A* **2003**, 107, 1112.
- (30) Hintze, P. E.; Feierabend, K. J.; Havey, D. K.; Vaida, V. *Spectrochim. Acta, Part A* **2005**, 61, 559.
- (31) Feierabend, K. J.; Havey, D. K.; Vaida, V. *Spectrochim. Acta, Part A* **2004**, 60, 2775.
- (32) Feierabend, K. J.; Havey, D. K.; Hintze, P. E.; Vaida, V. Private communication.
- (33) Natsheh, A. A.; Nadykto, A. B.; Mikkelsen, K. V.; Yu, F.; Ruuskanen, J. *J. Phys. Chem. A* **2004**, 108, 8914.
- (34) Vaida, V.; Kjaergaard, H. G.; Hintze, P. E.; Donaldson, D. J. *Science* **2003**, 299, 1566.
- (35) Miller, Y.; Chaban, G. M.; Gerber, R. B. *Chem. Phys.* **2005**, 313, 213.
- (36) Bowman, J. M. *J. Chem. Phys.* **1978**, 68, 608.
- (37) Bowman, J. M. *Acc. Chem. Res.* **1986**, 19, 202.
- (38) Gerber, R. B.; Ratner, M. A. *Adv. Chem. Phys.* **1988**, 70, 97.
- (39) Gerber, R. B.; Ratner, M. A. *Chem. Phys. Lett.* **1979**, 68, 195.
- (40) Jung, J. O.; Gerber, R. B. *J. Chem. Phys.* **1996**, 105, 10332.
- (41) Norris, L. S.; Ratner, M. A.; Roitberg, A. E.; Gerber, R. B. *J. Chem. Phys.* **1996**, 105, 11261.
- (42) Chaban, G. M.; Jung, J. O.; Gerber, R. B. *J. Chem. Phys.* **1999**, 111, 1823.
- (43) Chaban, G. M.; Jung, J. O.; Gerber, R. B. *J. Phys. Chem. A* **2000**, 104, 2772.
- (44) Wright, N. J.; Gerber, R. B. *J. Chem. Phys.* **2000**, 112, 2598.
- (45) Gregurick, S. K.; Chaban, G. M.; Gerber, R. B. *J. Phys. Chem. A* **2002**, 106, 8696.
- (46) Gerber, R. B.; Brauer, B.; Gregurick, S. K.; Chaban, G. M. *PhysChemComm* **2002**, 5, 142.
- (47) Chaban, G. M.; Gerber, R. B. *J. Chem. Phys.* **2001**, 115, 1340.
- (48) Chaban, G. M.; Jung, J. O.; Gerber, R. B. *J. Phys. Chem. A* **2000**, 104, 10035.
- (49) Wright, N. J.; Gerber, R. B.; Tozer, D. J. *Chem. Phys. Lett.* **2000**, 324, 206.
- (50) Chaban, G. M.; Gerber, R. B.; Janda, K. C. *J. Phys. Chem. A* **2001**, 105, 8323.
- (51) Chaban, G. M.; Gerber, R. B. *Spectrochim. Acta, Part A* **2002**, 58, 887.
- (52) Gerber, R. B.; Jung, J.-O. In *Computational Molecular Spectroscopy*; Jensen, P., Bunker, P. R., Eds.; Wiley: Chichester, U.K., 2000; p 365.
- (53) Carter, S.; Culik, S. J.; Bowman, J. M. *J. Chem. Phys.* **1997**, 107, 10458.
- (54) Brauer, B.; Chaban, G. M.; Gerber, R. B. *Phys. Chem. Chem. Phys.* **2004**, 6, 2543.
- (55) Gerber, R. B.; Chaban, G. M.; Gregurick, S. K.; Brauer, B. *Biopolymers* **2003**, 68, 370.
- (56) Matsunaga, N.; Chaban, G. M.; Gerber, R. B. *J. Chem. Phys.* **2002**, 117, 3541.
- (57) Benoit, D. M. *J. Chem. Phys.* **2004**, 120, 562.
- (58) Christiansen, O. *J. Chem. Phys.* **2004**, 120, 2140.
- (59) Pople, J. A.; Binkley, J. S.; Seeger, R. *Int. J. Quantum Chem.* **1976**, 10, 1.
- (60) Dunning, T. H. *J. Chem. Phys.* **1971**, 55, 716.
- (61) Wilson, E. B.; Decius, J. C.; Cross, P. C. *Molecular Vibrations*; McGraw-Hill: New York, 1995.
- (62) <http://www.msg.ameslab.gov/GAMESS/GAMESS.html>.
- (63) Kuczkowski, R. L.; Sueram, R. D.; Loves, F. J. *J. Am. Chem. Soc.* **1981**, 103, 2561.
- (64) Re, S.; Osamura, Y.; Morokuma, K. *J. Phys. Chem. A* **1999**, 103, 3535.
- (65) Fiocco, D. L.; Hunt, S. W.; Leopold, K. R. *J. Am. Chem. Soc.* **2002**, 124, 4504.
- (66) Havey, D. K.; Feierabend, K. J.; Vaida, V. *THEOCHEM* **2004**, 680, 243.
- (67) Brindle, C. A.; Chaban, G. M.; Gerber, R. B.; Janda, K. C. *Phys. Chem. Chem. Phys.* **2005**, 7, 945.